

# Variations of Air and Water Temperatures across and Along the Pads of Direct Evaporative Coolers and Their Effect on the Performance

M. Mosa<sup>#1</sup>, A. Saleh<sup>\*2</sup>

<sup>#</sup>Department of Mechanical Engineering, Faculty of Engineering, Aljouf University, Sakaka, Saudi Arabia

## Abstract

This paper presents the effect of variations of air and water temperatures across and along the pads of direct evaporative coolers and their effect on the performance. Two thicknesses of a (60cm × 76cm) pad are considered in this study. It is found that, for the thickness of 10 cm, variation of air temperature across the pad varies from 3.7 degrees at the top to 7.4 degrees at the bottom of the pad. For the thickness of 15 cm, variation of air temperature across the pad varies from 6.3 degrees at the top to 10.57 degrees at the bottom of the pad. It was found, also, that the profiles of the air temperature at the lower sectors of the pad are almost identical. The variation of water temperature across the pad was insignificant in the two cases considered. These results are used in optimization of the dimensions of the pad that maximize the performance of the cooler. The optimal thickness is restricted by the acceptable upper limit of relative humidity. It was found that with 70% relative humidity, the optimal thickness was 15 cm while with 85% relative humidity, the optimal thickness was 25 cm.

**Keywords:** direct evaporative cooler, cooler pad, heat and mass transfer, cooling efficiency.

## I. INTRODUCTION

Recently, environmental problems such as depletion of ozone layer and green house effects became serious problems. Studies have shown that the conventional working fluids of vapor compression systems are causing ozone layer depletion and green house effect. Therefore researches were devoted toward environmentally friendly systems such as absorption and evaporative cooling.

In evaporative coolers, as shown in Fig. 1, the cooling of air is achieved by the flow of air across a vertical porous pad while water flows from top to bottom. The non evaporated water is collected in a tray at the bottom of the pad and is re-circulated by a pump up to the top of the pad. Air flow is induced by a fan which draws in the outside air.

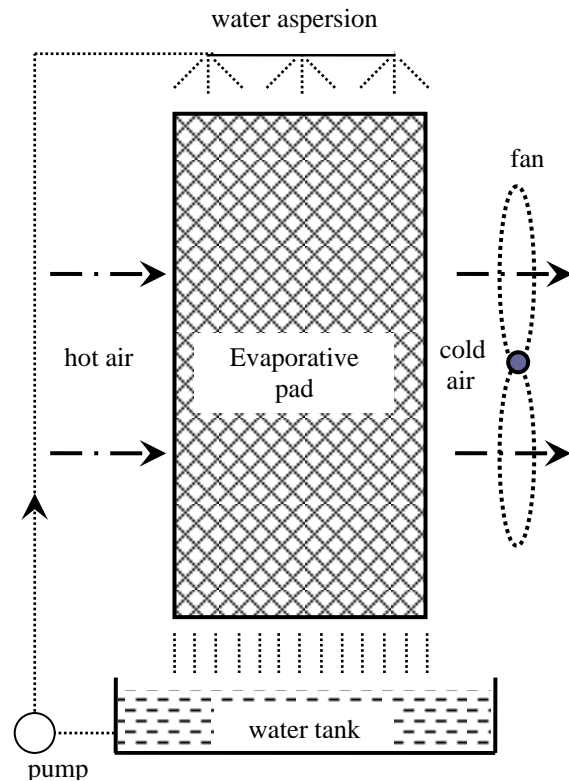


Fig. 1 Direct Evaporative Cooler

Kachhwaha and Parbhakar [1] presented a simple and efficient methodology to design a household desert cooler, predict performance of evaporative medium and determine pad thickness and height for achieving maximum cooling. Their theoretical results are in a good agreement with the experimental ones. Camarago et al. [2], [3] presented, theoretically and experimentally, the basic principle of the evaporative cooling process for human thermal comfort. Their results allow determination of the effectiveness of saturation and the convective heat transfer coefficient. Kulkarni and Rajput [4] made a theoretical performance analysis of three cooling pads of different materials for evaporative cooler. They observed that the saturation efficiency decreases with increase in mass flow rate of air, and the material with higher wetted surface area gives higher saturation efficiency.

Wu et al. [5] analyzed the heat and mass transfer between air and water film in direct evaporative cooler and proposed and validated experimentally a simplified cooling efficiency correlation. They discussed the influence of the air frontal velocity and the thickness of pad on the cooling efficiency. Sodha and Somwanshi [6] presented a model for the evaluation of the variation of water temperature along the direction of flow in an evaporating pad. They used the model to evaluate the mean air exit temperature and the transient temperature of the water in the tank. Their analytical results were in agreement with the experimental ones. Metin et al. [7] studied the relationship between the velocity of the air passing through the pad, the obtained decrease in the temperature of the air passing the pad and the cooling efficiency at the cellulose based evaporative cooling pad. They concluded that it was not possible to make a mathematical connection among velocities of the air passing through the pad, the obtained decrease of the air temperature and the cooling efficiency. However, it can be said that the most appropriate air velocity for the pad used in the test should be higher than  $0.5 \text{ ms}^{-1}$  and lower than  $1.5 \text{ ms}^{-1}$ . Dai et al. [8] investigated a cross-flow direct evaporative cooler, in which the wet durable honeycomb paper constituted the packing material. They developed a mathematical model, including the governing equations of liquid film and gas phases as well as the interface conditions, to predict the interface temperature of falling film. Wu et al. [9] developed a simplified mathematical model to describe the heat and moisture transfer between water and air in a direct evaporative cooler. They calculated and analyzed the influences of the inlet frontal air velocity, pad thickness, inlet air dry-bulb and wet-bulb temperatures on the cooling efficiency of the evaporative cooler.

All these analyses considered variation of air and water temperature along the pad and neglected the variation across the pad. In this study an attempt has been made to analyze the performance of evaporative coolers taking into account both the variation of temperature along and across the pad.

## II. MATHEMATICAL MODEL

Fig. 2 shows a pad of an evaporative cooler of height ( $H$ ), width ( $B$ ) and thickness ( $\delta$ ). Water flows down in the  $z$  direction while air flows in the  $x$  direction.

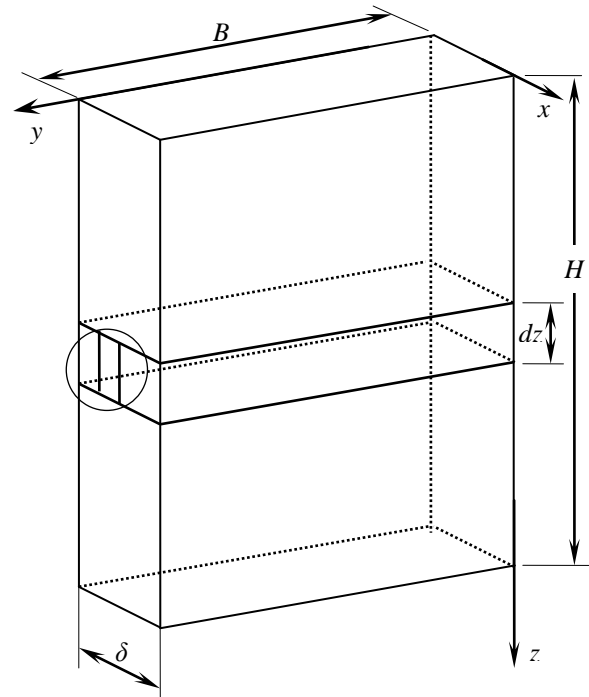


Fig. 2 Pad Configuration

The temperatures of the air ( $T_a = f(x,z)$ ) and water ( $T_w = f(z)$ ) inside the pad are related by [5]:

$$\frac{T_a - T_w}{T_{ao} - T_w} = e^{-\alpha x} \quad (1)$$

$$\text{where, } \alpha = \frac{h_c \xi}{\rho_a v_a c_{pa}}$$

$T_{ao}$ : is temperature of the inlet atmospheric air.

$\xi$ : is pore surface coefficient per unit pad volume.

$h_c$ : is the convective heat transfer coefficient between air and water.

$v_a$ : is the velocity of air.

$\rho_a$ : is the density of air.

$c_{pa}$ : is the air specific heat at constant pressure.

Substituting ( $x = \delta$ ) in Equation (1) and rearranging, the exit and the mean temperatures of air are given, respectively, by

$$T_{ae} = T_w (1 - e^{-\alpha \delta}) + T_{ao} e^{-\alpha \delta} \quad (2)$$

$$\bar{T}_{ae} = T_w + (T_{ao} - T_w) (1 - e^{-\alpha \delta}) / \alpha \delta \quad (3)$$

The energy balance of water, for the element of pad of thickness  $dz$  shown in Figure (1), may be expressed as [6]

$$\dot{m}_w c_w \frac{dT_w}{dz} dz + \dot{Q}_L dz + \dot{Q}_S dz = 0 \quad (4)$$

where  $\dot{Q}_L dz$  and  $\dot{Q}_S dz$  are the latent and the sensible heat transfer due to convection from water to air in the element of volume  $\delta B dz$ .

For unit Lewis number, the latent and the sensible heats are given by [10]:

$$\dot{Q}_L = 13 \times 10^{-3} h_c (P_w - \gamma P_a) \xi \delta B \quad (5)$$

and

$$\dot{Q}_S = h_c(T_w - T_a)\xi\delta B \quad (6)$$

Sodha & Somwanshi [6] correlated the table of saturation vapor pressure of water in [10] and, with aid of Equations (3), (4), (5), and (6), represented the exit and the mean (over z) temperatures of water flowing through the cooler pad, respectively, by

$$T_{we} = \frac{B'}{2A} + C_1 \left\{ \frac{1 + \beta e^{-2AC_1\lambda_0}}{1 - \beta e^{-2AC_1\lambda_0}} \right\} \quad (7)$$

$$\bar{T}_{we} = \frac{B'}{2A} + \frac{1}{A\lambda_0} \ln \left\{ \frac{e^{2AC_1\lambda_0} - \beta}{1 - \beta} \right\} - C_1 \quad (8)$$

Also, from (3) and (8) the average exit temperature of air is given by

$$\bar{T}_{ae} = e^{-\alpha\delta} (T_{a0} - \bar{T}_{we}) + \bar{T}_{we} \quad (9)$$

where

$$\lambda_0 = \left[ \frac{h_c \xi \delta B}{\dot{m}_w c_w} \right] H, \quad K_1 = \frac{1 - e^{-\alpha\delta}}{\alpha\delta},$$

$$A = 0.083, \quad B' = 1.76 - K_1$$

$$C = 0.083\gamma T_{a0}^2 + T_{a0}(K_1 - 1.76\gamma) + 32.7(\gamma - 1),$$

$$\beta = \frac{T_{w0} - (B'/2A) - C_1}{T_{w0} - (B'/2A) + C_1}, \quad C_1 = \sqrt{(B'/2A)^2 + C/A}$$

$T_{w0}$ : is the inlet temperature of water at the top of the pad.

### III. SIMULATION PROCEDURE

The above model doesn't take into account variations of air and water temperatures across the pad. To consider variations of air and water temperatures along the x axis (direction of air flow) and the z direction, the pad thickness is divided horizontally into (M) sectors and vertically into (N) sectors, i.e (M×N) segments. Each of these segments is treated individually as a separate pad. Fig. 3 shows one of these segments (i,j)<sup>th</sup>, of dimensions (Δx,B,dz), taken from the main pad shown in Fig. 2.

Exit air temperature from this segment becomes inlet temperature for the (i, (j+1))<sup>th</sup> segment, while exit water temperature becomes inlet temperature for the ((i+1),j)<sup>th</sup> segment.

$$\begin{cases} T_{a,in}^{(i,j+1)} = T_{a,out}^{(i,j)} \\ T_{w,in}^{(i+1,j)} = T_{w,out}^{(i,j)} \end{cases} \quad (10)$$

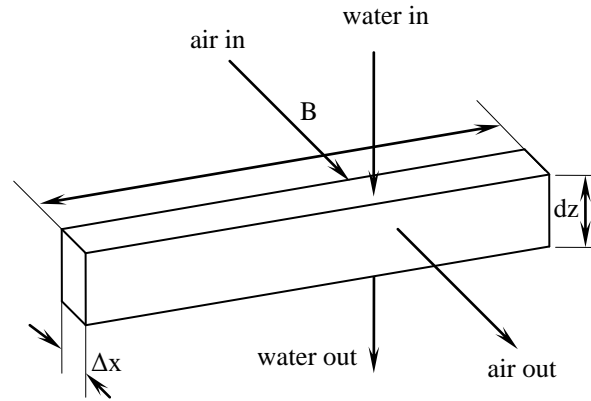


Fig. 3 Segment Configuration

The average temperature of the air, leaving the M horizontal sectors, is the sum of predicted outlet air temperatures over all horizontal sectors.

$$\bar{T}_{a,out} = \sum_{i=1}^M T_{a,out}^{(i,N)} \quad (11)$$

The average temperature of the water, leaving the N vertical sectors, is the sum of predicted outlet water temperatures over all vertical sectors.

$$\bar{T}_{w,out} = \sum_{j=1}^N T_{w,out}^{(i,M)} \quad (12)$$

For the pad selected for simulation, Wu et al. [9] determined experimentally the convective heat transfer coefficient as

$$h_c = 25.2v_a^{0.65} \quad (13)$$

and the cooling efficiency as

$$\eta = \frac{T_{a0} - \bar{T}_{ae}}{T_{a0} - T_{wb,0}} \times 100\% \quad (14)$$

where  $T_{wb,0}$  is the wet bulb temperature of air at inlet to the pad.

An algorithm using MATLAB was designed to solve this model with the aid of simulation parameters shown in TABLE I. The flow chart of the algorithm is shown in Fig. 4.

Table I Simulation Parameters

Air		$T_{w0}$	33 °C
$c_{pa}$	1005 J.kg <sup>-1</sup> .°C <sup>-1</sup>	$T_{a0}$	39.3 °C
$v_a$	1.66 ms <sup>-1</sup>	pad	
$\gamma$	0.335	$B$	0.6 m
$\rho_a$	1.2 kgm <sup>-3</sup>	$H$	0.76 m
Water		$\delta$	0.1 & 0.15 m
$c_w$	4200 J.kg <sup>-1</sup> .°C <sup>-1</sup>	$\xi$	440 m <sup>2</sup> m <sup>-3</sup>
$\dot{m}_w$	0.116 kg.s <sup>-1</sup>		

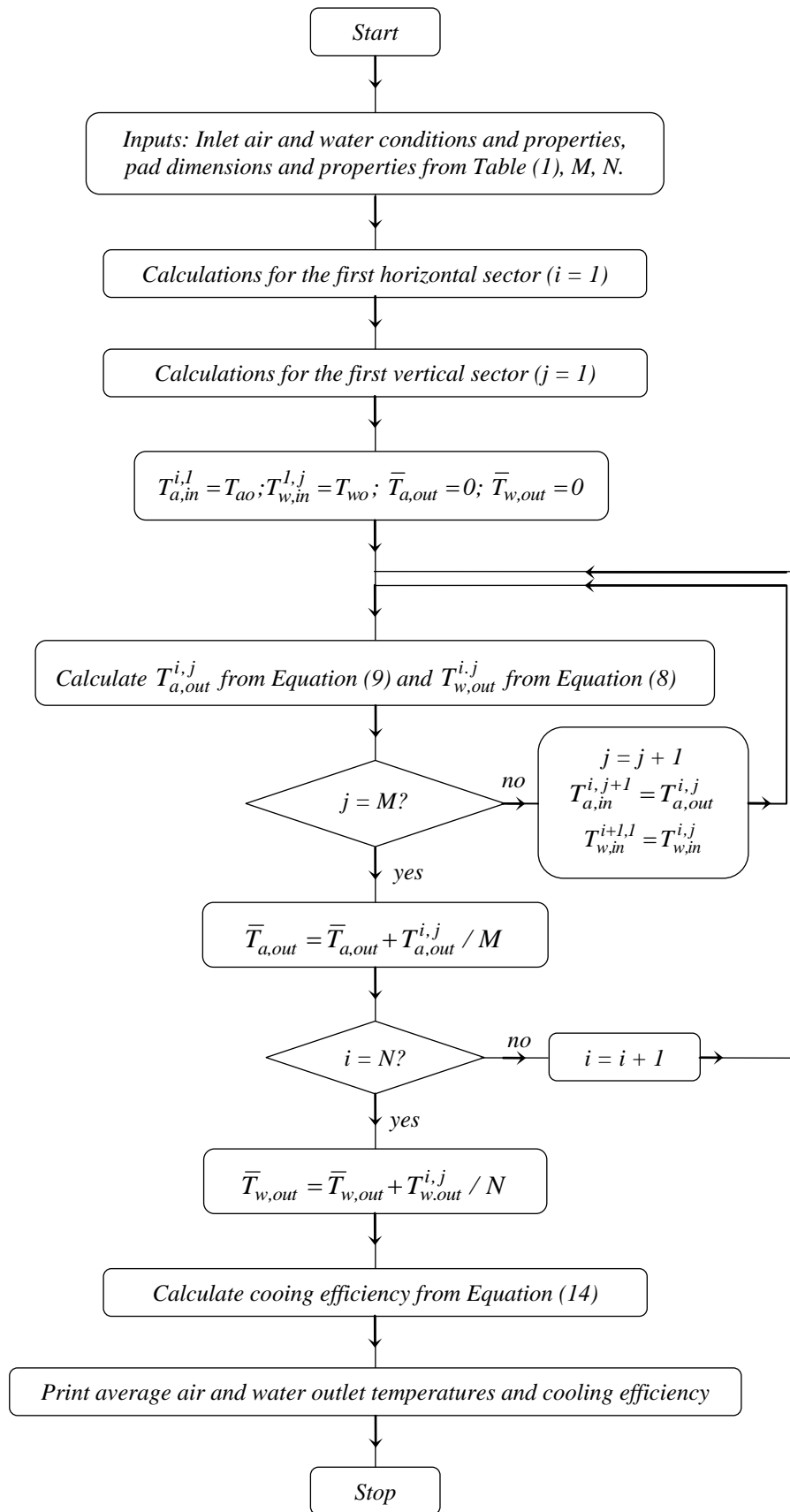


Fig. 4 Simulation Flow Chart

**IV. RESULTS AND DISCUSSION**

**A. Model Validation**

TABLE II presents air and water outlet temperatures and the effectiveness of the cooler for eight sets of horizontal ( $M$ ) and vertical ( $N$ ) sectors of the pad thickness 10 cm. The results that appears for the first set,  $M \times N = 10 \times 10$ , ( $\bar{T}_{ae} = 31.90^\circ C$ ,  $\bar{T}_{we} = 24.85^\circ C$ ) agrees very well with experimental results ( $\bar{T}_{ae} = 30.8^\circ C$ ,  $\bar{T}_{we} = 24.9^\circ C$ ) presented by Sodha & Somwanshi [6]. The best result in which achieved the minimum air temperature is the seventh set ( $M \times N = 10 \times 1$ ).

**Table II : Air And Water Exit Temperatures For Different Vertical And Horizontal Sectors Sets ( $\Delta = 10$  Cm)**

$M \times N$	$\bar{T}_{ae}$	$\bar{T}_{we}$	$\eta$
10×10	31.90	24.85	0.5331
5×10	31.95	25.01	0.5295
2×10	32.12	25.52	0.5173
1×10	32.42	26.36	0.4957
10×5	31.73	24.95	0.5454
10×2	31.36	25.27	0.5720
10×1	30.99	25.79	0.5987
1×1	31.85	27.18	0.5367

**B. Variation of Air and Water Temperatures Along and Across a 10 cm Pad**

Fig. 5 shows the variation of air temperature across and along a 10 cm thickness pad for (10×10) segments. It can be noticed that the best cooling occurs at the lower part of the pad. Also, it can be noticed that through the lowermost sectors of the pad, the exit air temperature profiles are almost identical. The maximum drop through the lowest set of sectors

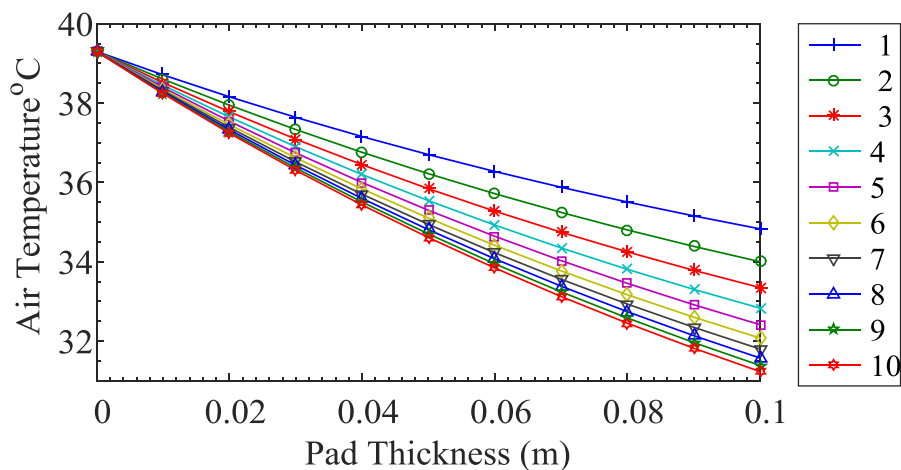


**Fig. 5 Variation of Air Temperature Across the Ten Horizontal Sectors**

is around 7.4 degrees. These results can be used for optimizing the dimension of the cooling pads.

Fig. 6 shows the variation of water temperature across and along the pad for the thickness 10 cm. It can be seen that variation of water temperature across the pad is insignificant with a range of about 1.9% at the top and 4.4% at the bottom. On the other hand a significant drop can be noticed along the pad. The temperature drop exceeded 8 degrees along the first vertical set of sectors and came close to 10 degrees along the last vertical set of sectors.

**C. Variation of Air and Water Temperatures Along and Across a 15 cm Pad**

TABLE III presents air and water outlet temperatures and the effectiveness for eight sets of horizontal ( $M$ ) and vertical ( $N$ ) sectors for a pad thickness of 15 cm. Also in this case the minimum water temperature was achieved with the first set and the minimum air temperature was achieved with the seventh set.

**Table III : Air And Water Exit Temperatures For Different Vertical And Horizontal Sectors Sets ( $\Delta = 15$  Cm)**

$M \times N$	$\bar{T}_{ae}$	$\bar{T}_{we}$	$\eta$
10×10	28.73	22.73	0.7615
5×10	28.86	23.05	0.7522
2×10	29.27	23.79	0.7226
1×10	30.26	25.53	0.6513
10×5	28.45	22.88	0.7817
10×2	27.90	23.26	0.8213
10×1	27.46	23.98	0.8530
1×1	29.41	26.27	0.7125

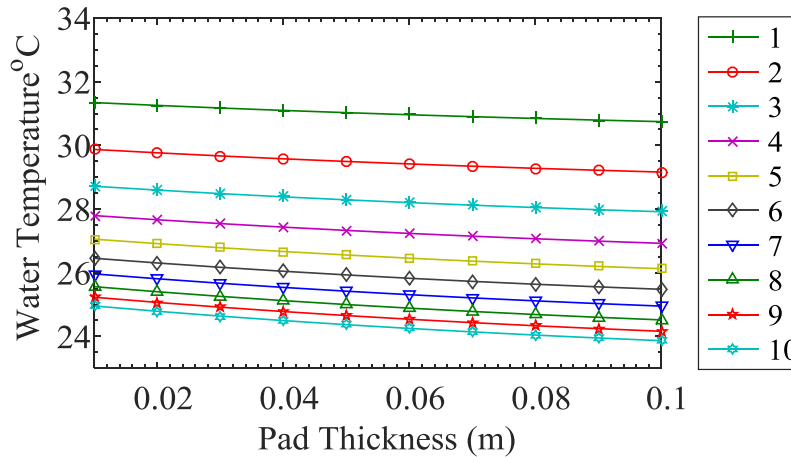


Fig. 6 Variation of Water Temperature Across the Ten Horizontal Sectors

Fig. 7 shows the variation of air temperature across and along the pad of thickness 15 cm for (10×10) segments. Again it can be noticed that the best cooling occurs at the lower part of the pad with temperature profiles through the last sectors of the pad almost identical. In this case, the maximum drop through the lowest set of sectors is larger; it exceeded 10.5 degrees.

This means that an improvement in cooling efficiency took place with the increased thickness of pad.

An important idea can be extracted from these results if the outlet of cooler is modified such as to be divided into two sections. A lower section that provides a low temperature of air and this can be connected to the conditioned space. An upper section with a relatively higher temperature of air and this can be re-circulated and used to cool indirectly the supplied air. This modification will lead to an improvement in cooling efficiency due to the lower average air temperature of the supplied air.

This modification will reduce the mass flow rate of supplied air, but this shortage can be compensated by an adequate selection of the blower. This modification is beyond the scope of this study.

Fig. 8 shows the variation of water temperature across and along a pad of thickness 15 cm (10×10) segments. It can be seen that variation of water temperature across the pad is in the range of 3.8% at the top sector to 9.3% at the bottom sector. In this case the temperature drop along the last vertical set of sectors came close to 12 degrees. This means that a higher temperature drop in water temperature took place with the increased pad thickness.

**D. Optimization of the Dimensions of the Pad**

The effect of the pad height on air temperature seems to be remarkable in the upper sectors but diminished to become insignificant through the lower sectors as shown in Fig. 5 and 7. On the other hand, the effect of pad thickness is notable as can be sown in the same figures.

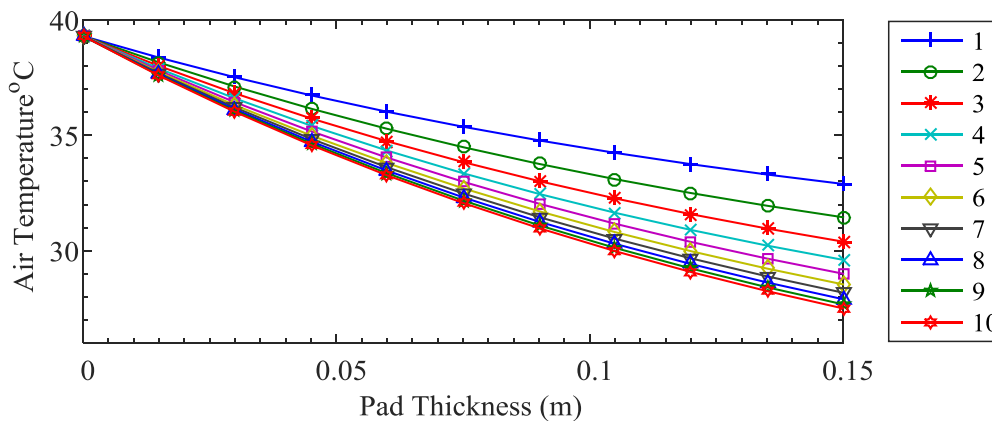


Fig. 7 Variation of Air Temperature Across the Ten Horizontal Sectors

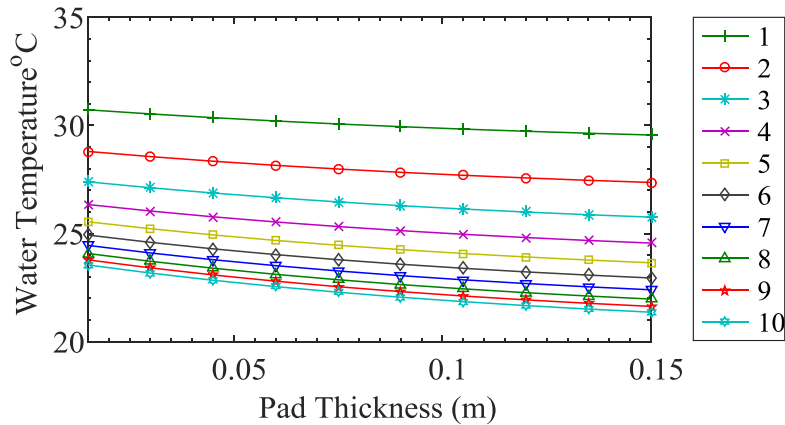


Fig. 8 Variation of Water Temperature Across the Ten Horizontal Sectors

In Fig. 9a the variation of average air temperature leaving the pad with pad thickness is presented. It can be noticed that the drop in air temperature takes place initially with high rate to decrease gradually with the thickness. A similar trend but with an increasing rate can be noticed for cooling efficiency as shown in Fig. 9b. There are some restrictive factors that prevent reaching the optimum thickness that achieves the minimum temperature. The economic factor and the increased pressure drop can

be easily addressed. These factors are beyond the scope of this study. The most critical barrier is the increased relative humidity that can exceed the acceptable comfortable conditions. The variation of relative humidity with pad thickness is shown in Fig. 9c. It can be noticed that to keep the relative humidity less than 70%, the thickness of the pad should not exceed 15 cm with an air outlet temperature around 29 degrees.

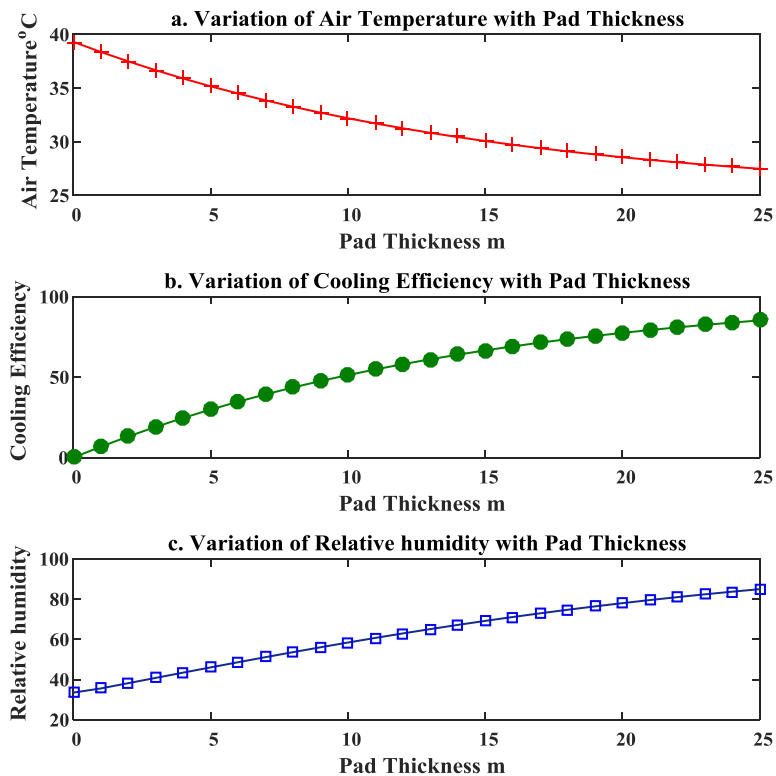


Fig. 9 Variation of Air Temperature, Cooling Efficiency and Relative Humidity with Pad Thickness

In other circumstances in which a higher relative humidity can be accepted, other optimum thickness values may be found that achieve a lower air

temperature. For example, as can be shown in Figure 9, accepting a relative humidity around 85% corresponds

to an optimal pad thickness around 25 cm and provides a leaving air temperature around 27 degrees.

### V. CONCLUSION

The objective of this study is to investigate variations of air and water temperature along and across the pad of evaporative coolers and their effect on the performance. According to this study, the following conclusions can be drawn:

- For pad thickness of 10cm variation of air temperature across the pad varies from 3.7 degrees at the top to 7.4 degrees at the bottom of the pad
- For the thickness of 15 cm, variation of air temperature across the pad varies from 6.3 degrees at the top to 10.57 degrees at the bottom of the pad.
- Air outlet temperature profile at the lower sectors of the pad is almost identical. This means that the effect of the pad height is almost negligible beyond the sixth sector.
- For thin pads, variation of water temperature across the pad can be neglected with no significant error in air and water outlet temperatures.
- Relative humidity plays an important role in evaluation of the optimized thickness of the pad; when the upper limit of relative humidity was fixed at 70%, the optimal thickness was 15 cm and when the upper limit of relative humidity was fixed at 85%, optimal thickness was 25 cm.
- With an optimal thickness value of 15 cm the air temperature drop approached 10 degrees and the cooling efficiency exceeded 66%.
- With an optimal thickness value of 25 cm the air temperature drop approached 12 degrees and the cooling efficiency exceeded 85%.

### NOMENCLATURE

$B$	Width of pad (m).
$c_{pa}$	Specific heat of air at constant pressure ( $J.kg^{-1}.^{\circ}C^{-1}$ ).
$c_w$	Specific heat of water ( $J.kg^{-1}.^{\circ}C^{-1}$ ).
$H$	Height of pad (m).
$h_c$	Convective heat transfer coefficient between air and water ( $Wm^{-2}.^{\circ}C^{-1}$ ).
$\dot{m}_w$	Mass flow rate of water ( $kgs^{-1}$ ).
$P_a$	Saturated water vapor pressure in air ( $Nm^{-2}$ ).
$P_w$	Saturated water vapor pressure in air at the temperature of water ( $Nm^{-2}$ ).
$\dot{Q}_L$	Latent heat (W).
$\dot{Q}_S$	Sensible heat (W).
$T_{ae}$	Temperature of the exit air ( $^{\circ}C$ ).
$\bar{T}_{ae}$	Mean (over x) temperature of air ( $^{\circ}C$ ).

$T_{a0}$	Temperature of inlet atmospheric air ( $^{\circ}C$ ).
$T_{we}$	Exit water temperature of the water ( $^{\circ}C$ ).
$\bar{T}_{we}$	Mean temperature (over z) of water flowing through pad ( $^{\circ}C$ ).
$T_{w0}$	Temperature of the water at the top of evaporative pad ( $^{\circ}C$ ).
$v_a$	Velocity of air ( $ms^{-1}$ ).
<i>Greek letters</i>	
$\delta$	Thickness of pad (m).
$\eta$	Cooling efficiency.
$\xi$	Pore surface coefficient per unit pad volume ( $m^2m^{-3}$ ).
$\gamma$	Relative humidity of air.
$\rho_a$	Density of air ( $kgm^{-3}$ ).

### REFERENCES

- [1] S. S. Kachhwaha and Suhas Prabhakar, "Heat and mass transfer study in a direct evaporative cooler," Journal of Scientific & Industrial Research, vol. 69, pp. 705-710, 2010.
- [2] Jose´ Rui Camargo, Carlos Daniel Ebinumab and Jose´ Luz Silveirab. "Experimental performance of a direct evaporative cooler operating during summer in a Brazilian city," International Journal of Refrigeration, vol. 28, pp. 1124–1132, 2005.
- [3] J. R. Camargo, D. C. Ebinuma and S. Cardoso, "A mathematical model for direct evaporative cooling air conditioning system," Engenharia Térmica, vol. 3, pp. 30-34, 2003.
- [4] R. K. Kulkarni and S. P. S. Rajput, "Comparative performance of evaporative cooling pads of alternative materials," International Journal of Advanced Engineering Sciences and Technologies (IAEST), vol. 10(2), pp. 239-244, 2011.
- [5] J. M. Wu, X. Huang and H. Zhang, "Theoretical analysis on heat and mass transfer in a direct evaporative cooler," Applied Thermal Engineering, vol. 29, pp. 980-984, 2009.
- [6] M. S. Sodha and A. Somwanshi, "Variation of water temperature along the direction of flow: effect on performance of an evaporative cooler," Journal of Fundamentals of Renewable Energy and Applications, vol. 2, pp 1-6, 2012.
- [7] Metin Dagtekin, Cengiz Karaca, Y. ilmaz Yildiz, Ali Bascetinçelik and Ömer Paydak, "The effects of air velocity on the performance of pad evaporative cooling systems," African Journal of Agricultural Research, vol. 6(7), pp. 1813-1822, 2011.
- [8] Y. J. Dai and K. Sumathy, "Theoretical study on a cross-flow direct evaporative cooler using honeycomb paper as packing material," Applied Thermal Engineering, vol. 22, pp. 1417–1430, 2002.
- [9] J. M. Wu, X. Huang and H. Zhang, "Numerical investigation on the heat and mass transfer in a direct evaporative cooler," Applied Thermal Engineering, vol. 29, pp. 195–201, 2009.
- [10] G. N. Tiwari, Solar Energy Fundamentals, Design Modelling and Applications, New Delhi, India: Narosa Publishing House, 2002.